

“Sponge Crystal”: a novel class of microporous single crystals formed by self-assembly of polyoxometalate $(\text{NH}_4)_3\text{PW}_{12}\text{O}_{40}$ nanocrystallites

Kei Inumaru*

Department of Applied Chemistry, Graduate School of Engineering, Hiroshima University, Higashi-Hiroshima 739-8527, Japan

In this account, a new concept of “sponge crystals” is presented on the basis of new interpretation of our previous results of porous heteropolyacids, that is, porous aggregates of self-assembled $(\text{NH}_4)_3\text{PW}_{12}\text{O}_{40}$ nanocrystallites (Ito, Inumaru, and Misono, *J. Phys. Chem. B* 101 (1997) 9958; *Chem. Mater.* 13 (2001) 824) “Sponge crystals” are defined as single crystals having continuous voids within them, but unlike zeolites, no intrinsic structural pores. This new category includes molecular single crystals having continuous voids originating from series of neighboring vacancies (≥ 1 nm) of the constituent large molecules, affording nanospaces in the crystals. A typical example of “sponge crystals” is $(\text{NH}_4)_3\text{PW}_{12}\text{O}_{40}$, which is formed via the dropwise addition of ammonium hydrogen carbonate into an $\text{H}_3\text{PW}_{12}\text{O}_{40}$ aqueous solution (titration method) at 368 K. The resulting $(\text{NH}_4)_3\text{PW}_{12}\text{O}_{40}$ nanocrystallites (ca. 6–8 nm) then self-assemble with the same crystal orientation to form porous dodecahedral aggregates in the solution. During the formation process, necks grow epitaxially between the surfaces of the nanocrystallites (“Epitaxial Self-Assembly”) to form aggregates of which each aggregate has an ordered structure as a whole single crystal. Although the crystal structure of $(\text{NH}_4)_3\text{PW}_{12}\text{O}_{40}$ has no intrinsic structural (“built-in”) pores, X-ray diffraction, electron diffraction and gas adsorption experiments all reveal that each $(\text{NH}_4)_3\text{PW}_{12}\text{O}_{40}$ aggregate is comprised of a single crystal bearing many micropores. These pores are considered to be continuous spaces as neighboring vacancies of the molecules (anions and cations) originating from the residual spaces between the self-assembled nanocrystallites. The porous $(\text{NH}_4)_3\text{PW}_{12}\text{O}_{40}$ single crystals are considered a special case of “mesocrystals,” as was recently discussed by Cölfen and Antonietti (*Angew. Chem. Int. Ed.* 44 (2005) 5576). In contrast to most “mesocrystals,” which are generally polycrystalline in nature, each aggregate of $(\text{NH}_4)_3\text{PW}_{12}\text{O}_{40}$ is a characteristic porous single crystal. Furthermore, the micropores of $(\text{NH}_4)_3\text{PW}_{12}\text{O}_{40}$ are totally different from those found in other microporous crystals: zeolites have “built-in” pores defined by their crystal structure, while the $(\text{NH}_4)_3\text{PW}_{12}\text{O}_{40}$ nanocrystallites have none. Since $(\text{NH}_4)_3\text{PW}_{12}\text{O}_{40}$ micropores are continuous spaces as neighboring vacancies of the molecules, the shapes of the $(\text{NH}_4)_3\text{PW}_{12}\text{O}_{40}$ pores can in principle, assume various connectivities or networks within the crystal, and as such, are subsequently termed: “sponge crystals.”

KEY WORDS: self-assembly; epitaxial self assembly; mesocrystal; heteropolyacid; porous crystal.

1. Introduction

Self-assembly of nanoparticles is a major topic of interest due to their prominent role in a number of promising processes for nanotechnology [1, 2]. “Colloidal crystals,” which have wide application as novel porous materials and photonic crystals, are among the latest of these topics [3–6]. Of such self-assembled aggregates, these properties are tunable by the type of clusters and the manner of their assembly. The control of these nanostructures is also important for the development of catalysts [7] and porous materials [8].

Heteropoly acids and their salts (heteropolyoxometalates) have attracted much attention during the last three decades owing to the versatilities of these compounds as catalytic materials [9–12]. These compounds comprise polyanions having well-defined structures and sizes of nanometer-scale. Among these compounds, $\text{H}_3\text{PM}_{12}\text{O}_{40}$ ($M = \text{W}$ or Mo) and their salts, which have Keggin-type polyanions, are most extensively

studied as catalytic materials for oxidation and acid-catalyzed reactions of organic compounds. Partially sulfated Cs salts were reported to show excellent acid catalytic properties tunable by changing the Cs content [13–16]. This material changes from mesoporous to microporous depending on the Cs content. An important consequence of this phenomenon is that this material can be tuned to exhibit molecular shape-selective catalysis [16]. In this material, the nanocrystallites and the way they aggregate, play an important role in the tunable porosity and the characteristic catalysis [15].

In our previous reports, we revealed that $(\text{NH}_4)_3\text{PW}_{12}\text{O}_{40}$ nanocrystallites self-assembled with the same crystal orientation to form porous dodecahedral aggregates. Moreover, necks between the crystallites were found to grow epitaxially during the formation process, enabling the nanocrystallites to form strong connection with each other; a phenomenon we defined as “Epitaxial Self Assembly” [17–23], as shown in figure 1. In this non-classical crystallization mechanism, the nanocrystallites form in supersaturated solutions, aggregating in an ordered manner, gaining higher crystallinity in the process. The epitaxially grown necks

*To whom correspondence should be addressed.
E-mail: inumaru@hiroshima-u.ac.jp

between the nanocrystallites form through local dissolution and reprecipitation.

Recently, Cölfen and Antonietti published a review outlining the concept of "mesocrystals," describing them as basically large aggregates formed by the ordered assembly of inorganic nanocrystallites [24]. This review provides a comprehensive interpretation of this phenomenon, which has only previously been described in the literature on a fragmentary basis. In their review, they describe "mesocrystals" as oriented superstructures of nanocrystals with common outer faces, formed from nonspherical, crystalline building units. They categorized the $(\text{NH}_4)_3\text{PW}_{12}\text{O}_{40}$ dodecahedron as an example of "mesocrystals" in terms of the formation process.

On the other hand, in terms of the structure of the final product, $(\text{NH}_4)_3\text{PW}_{12}\text{O}_{40}$ exhibits remarkable characteristics as a microporous material, distinguishing it from all other "mesocrystals" and usual microporous crystals (e.g. zeolites). These extraordinary characteristics are closely related to the fact that the $(\text{NH}_4)_3\text{PW}_{12}\text{O}_{40}$ consist of large molecules (polyanions).

This account presents a new additional interpretation of the previous results and shows that $(\text{NH}_4)_3\text{PW}_{12}\text{O}_{40}$ represents a novel class of porous single crystals, which we defines as "sponge crystals." The relationship among the concepts of "mesocrystals," usual microporous crystals (like zeolites), and the new category of "sponge crystals" will be discussed.

2. Porous partially sulfated $\text{Cs}_x\text{H}_{3-x}\text{PW}_{12}\text{O}_{40}$ reported before the study on the "epitaxial self assembly"

Since the 1980's, Okuhara and Misono *et al.* have reported the pronounced solid acid-catalysis of $\text{Cs}_x\text{H}_{3-x}\text{PW}_{12}\text{O}_{40}$. These catalysts were applied to liquid-solid systems as well as to gas-solid systems for reactions of various organic compounds [9, 10]. When $x = 2.5$, the corresponding salt has a large surface area ($\sim 135 \text{ m}^2 \text{ g}^{-1}$) and a maximized surface amount of acid sites affording high catalytic activity [13–15]. The Cs salts show remarkable catalytic activity even in aqueous solution [25]. The Cs salt is comprised of nanocrystals (6–8 nm), which aggregate to form structures showing mesoporosity.

Okuhara, Nishimura, and Misono discovered that $\text{Cs}_x\text{H}_{3-x}\text{PW}_{12}\text{O}_{40}$ exhibits tunable, molecular shape-selective catalysis. When $x = 2.1\text{--}2.2$, the resulting salt becomes microporous. An important consequence of this phenomenon is that $\text{Cs}_x\text{H}_{3-x}\text{PW}_{12}\text{O}_{40}$ can be tuned to exhibit remarkable molecular shaped-selective catalysis [16]. Later, Okuhara designed molecular shape-selective bifunctional catalysts for alkane isomerization by combining Cs salts with Pt [26,27]. On the basis of precise determinations of the pore diameter and pore volume, they concluded that micropores exist between

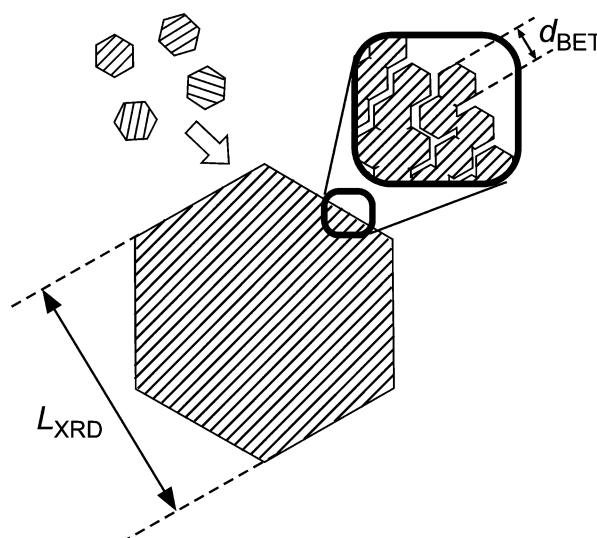


Figure 1. Schematic illustration of "epitaxial self-assembly" of $(\text{NH}_4)_3\text{PW}_{12}\text{O}_{40}$ nanocrystallites to form porous dodecahedral single crystals. d_{BET} is "particle diameter" calculated from surface area. L_{XRD} represents the length of the ordered structure as a single crystal determined from the X-ray diffraction line-width using Scherrer's equation. $(\text{NH}_4)_3\text{PW}_{12}\text{O}_{40}$ has L_{XRD} much larger than d_{BET} .

the crystal faces of the primary nanocrystallites, and that the spaces between them are formed as a result of crystallographic misfits between the nanocrystallites [28–37].

3. Studies on $(\text{NH}_4)_3\text{PW}_{12}\text{O}_{40}$ before the discovery of its "epitaxial self assembly"

Almost 30 years ago, Gregg *et al.* discovered that $(\text{NH}_4)_3\text{PW}_{12}\text{O}_{40}$ is microporous: They performed a series of gas adsorption studies on $(\text{NH}_4)_3\text{PW}_{12}\text{O}_{40}$ and speculated that the micropores exist in the crystals rather than between the grains, on the basis of their observations that the change in porosity was small when the sample powder was compacted into pellets [38]. Later, Moffat *et al.* measured the pore diameter distribution of $(\text{NH}_4)_3\text{PW}_{12}\text{O}_{40}$ and other salts prepared at ambient temperature [39,40], and from the corresponding X-ray powder diffraction patterns, claimed that $(\text{NH}_4)_3\text{PW}_{12}\text{O}_{40}$ and other porous salts give relative peak intensities much different from those of non-porous salts. They then went on to propose that the transformation of the crystal structure was responsible for the generation of micropore channels in $(\text{NH}_4)_3\text{PW}_{12}\text{O}_{40}$ and other porous salts. However, $(\text{NH}_4)_3\text{PW}_{12}\text{O}_{40}$ gives relative peak intensities that are very similar to those calculated from the known crystal structure, indicating no crystal structural change [17]. $(\text{NH}_4)_3\text{PW}_{12}\text{O}_{40}$ has a densely-packed structure with no interstitial spaces or "built-in" pores like zeolites. Therefore, the origin of microporosity in this material was a mystery before the discovery of "epitaxial self-assembly" (figure 1).

4. Porous aggregates of $(\text{NH}_4)_3\text{PW}_{12}\text{O}_{40}$ formed by epitaxial self assembly of nanocrystallites using the titration method [17–20]

In this section, we discuss the structure of $(\text{NH}_4)_3\text{PW}_{12}\text{O}_{40}$ prepared by the titration method. An aqueous solution of $(\text{NH}_4)\text{HCO}_3$ was added dropwise to an $\text{H}_3\text{PW}_{12}\text{O}_{40}$ aqueous solution at 298–368 K. Figures 2a and b shows a scanning electron microscopy (SEM) image of $(\text{NH}_4)_3\text{PW}_{12}\text{O}_{40}$ prepared at 368 K. The observed particles all had the same symmetrical dodecahedral shape (400–800 nm in size). Since the dodecahedra originally consist of small nanocrystallites (ca. 6–8 nm), their surfaces show a distinct roughness. Atomic force microscopy (AFM) images revealed that the small nanocrystallites were arrayed in a regular manner [20]. Figure 2c shows a selected area electron diffraction (ED) pattern of the entire dodecahedron. The experiment gave spotted pattern, confirming that the constituent nanocrystallites in the dodecahedron had the same crystal orientation.

Figure 3 shows the nitrogen adsorption–desorption isotherms of $(\text{NH}_4)_3\text{PW}_{12}\text{O}_{40}$ prepared at various temperatures. The resulting data demonstrated that the as-formed $(\text{NH}_4)_3\text{PW}_{12}\text{O}_{40}$ dodecahedra were microporous. The physical properties of these $(\text{NH}_4)_3\text{PW}_{12}\text{O}_{40}$ dodecahedra are listed in table 1. For the $(\text{NH}_4)_3\text{PW}_{12}\text{O}_{40}$ sample prepared at 368 K, the porosity was ca. 15%, while the total pore volume and BET surface area were $0.027 \text{ cm}^3 \text{ g}^{-1}$ and $65 \text{ m}^2 \text{ g}^{-1}$, respectively. Compared to zeolites, these values for the $(\text{NH}_4)_3\text{PW}_{12}\text{O}_{40}$ are lower, due to the heavy molecular weight of the polyanions (~ 2880).

The experimentally-obtained X-ray powder diffraction pattern (peak positions and relative intensities) of $(\text{NH}_4)_3\text{PW}_{12}\text{O}_{40}$ was very similar to the pattern computed from the known structure of $(\text{NH}_4)_3\text{PW}_{12}\text{O}_{40}$. Consequently, the obtained $(\text{NH}_4)_3\text{PW}_{12}\text{O}_{40}$ has a well-known cubic non-porous crystal structure, in which the polyanions are densely packed in a body-centered cubic (bcc) arrangement [17]. From the peak width of the diffraction, the length of the ordered structure can be calculated in terms of X-ray diffraction (L_{XRD}) using the following Scherrer’s equation:

$$L_{\text{XRD}} = 0.9\lambda / B \cos \theta$$

where λ is the wavelength of Cu $K\alpha$ radiation, B is the calibrated half-width of the (222) peak in radian, and θ is the diffraction angle of the (222) peak.

L_{XRD} represents the length in which an ordered crystal structure continues as a single crystal, as illustrated in figure 1.

Figure 4 shows the L_{XRD} value for the samples prepared at various temperatures (i.e. the temperature of the solution when the samples precipitated). Here, it was observed that L_{XRD} becomes greater as the preparation temperature increased from room temperature to 368 K.

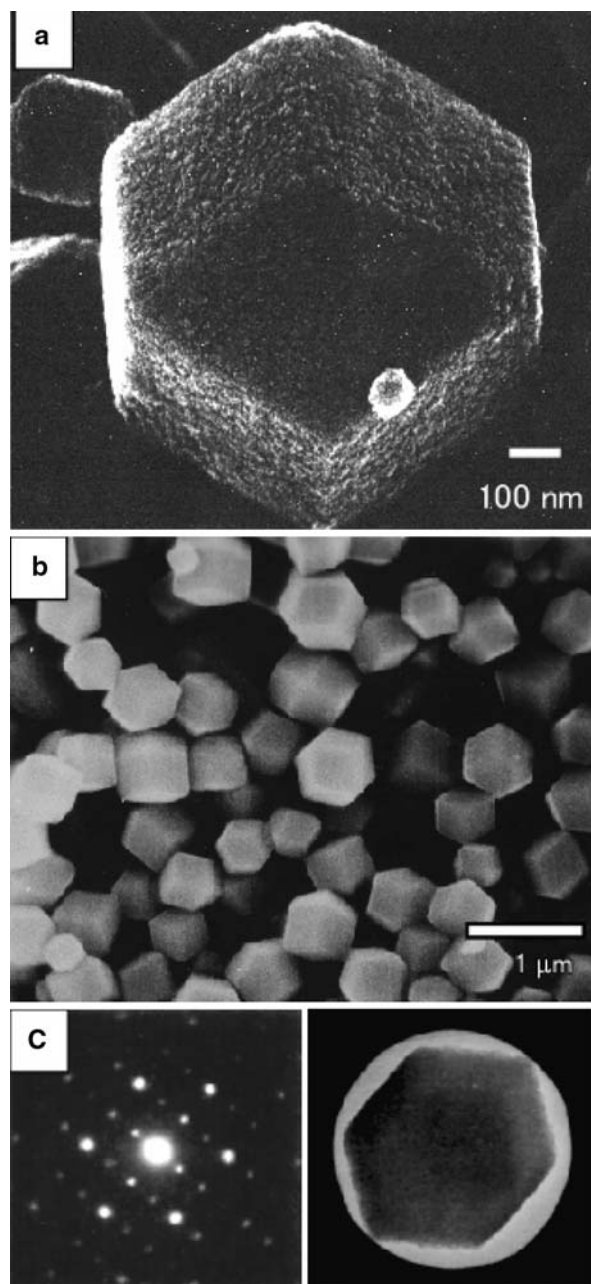


Figure 2. (a) and (b), SEM image of $(\text{NH}_4)_3\text{PW}_{12}\text{O}_{40}$ precipitated at 368 K via the titration method. Self assembly of the $(\text{NH}_4)_3\text{PW}_{12}\text{O}_{40}$ nanocrystallites affords porous dodecahedra of which each aggregate has an ordered structure as a whole single crystals, as confirmed by X-ray and electron diffraction studies. (c) Selected area electron diffraction of an $(\text{NH}_4)_3\text{PW}_{12}\text{O}_{40}$ dodecahedron. The spotted diffraction confirmed that the constituent nanocrystallites in the dodecahedron had the same crystal orientation. (a) and (c) are reproduced from ref 18 with permission of the Chemical Society of Japan.

Indeed, for $(\text{NH}_4)_3\text{PW}_{12}\text{O}_{40}$ prepared at 368 K, the L_{XRD} value calculated was 150 nm, which is more than 10 times larger than the size of the constituent nanocrystallites. The size of the nanocrystallites can be estimated on the basis of the BET surface area. Assuming a spherical shape for simplicity, the nanocrystallite diameters were calculated (designated by d_{BET}) as shown

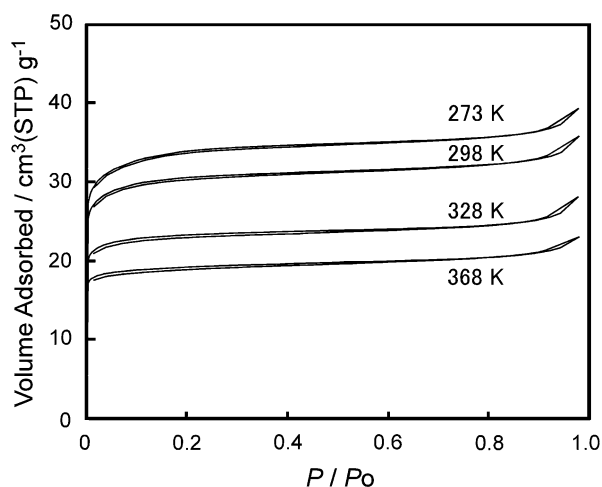


Figure 3. Nitrogen adsorption isotherms at 77 K for $(\text{NH}_4)_3\text{PW}_{12}\text{O}_{40}$ precipitated via the titration method at various temperatures.

in figure 4. The obtained $L_{\text{XRD}}/d_{\text{BET}}$ ratios were significantly larger than unity, and increased up to 9.9 as the preparation temperature was increased (table 1). This demonstrates that the constituent nanocrystallites are coherent in X-ray diffraction for much longer distances than the size of the nanocrystallites. This fact requires that necks grow epitaxially (by the local dissolution–reprecipitation process) between the surfaces of the nanocrystallites, and the extent of this epitaxial growth is high at higher temperatures, resulting in aggregates of nanocrystallites that become more like a continuous crystal. L_{XRD} and d_{BET} are considered to represent the dimensions of the aggregates and the constituent nanocrystallites, respectively (figure 1). The L_{XRD} for the sample prepared at 368 K was 150 nm and is comparable to the size of the dodecahedra in figure 2 (ca 400 nm), where the smaller L_{XRD} values may be due to the limitation of Scherrer's equation for large crystals. As was mentioned above, selected area electron diffraction (ED) patterns confirmed that the constituent nanocrystallites in the dodecahedron had the same crystal orientation (figure 2c). All of these results demonstrate that the dodecahedra are microporous single crystals with ordered structures.

Table 1
Properties of $(\text{NH}_4)_3\text{PW}_{12}\text{O}_{40}$ prepared by the titration method (Ref. 17)

Preparation temperature (K)	BET surface area ($\text{m}^2 \text{g}^{-1}$)	d_{BET} (nm)	Micropore volume ($10^{-2} \text{cm}^3 \text{g}^{-1}$)	L_{XRD} (nm)	$L_{\text{XRD}} / d_{\text{BET}}$
368	65	15	2.7	150 ^a	9.9
328	79	12	3.2	47	3.6
298	104	9	4.1	31 ^a	3.3
273	116	9	4.3	25	2.9

^aMeasured in the presence of moisture.

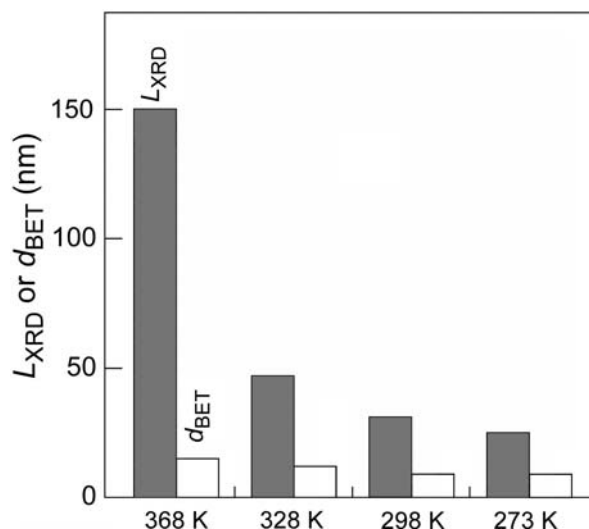


Figure 4. Comparison between the lengths of the ordered structure as a single crystal determined from the X-ray diffraction line-width (L_{XRD}), and crystallite size calculated from the BET surface areas (d_{BET}). The L_{XRD} values are significantly larger than the corresponding d_{BET} values, demonstrating that the nanocrystallites are connected by necks epitaxially grown between the faces of the crystallites.

The origin of the micropores is explained as residual spaces between the constituent nanocrystallites. The micropore diameter was analyzed by the Horvath–Kawazoe method using Ar adsorption, as shown in figure 5. Here, the $(\text{NH}_4)_3\text{PW}_{12}\text{O}_{40}$ peak is located between those of the two reference zeolites, H-ZSM-5 and H-Y. H-ZSM-5 possesses channels with diameters of 0.5–0.6 nm, while H-Y has supercages (diameter 1.3 nm), connected by short channels (0.7 nm in diameter). Since the total volume of the supercages is much larger than that of the channels, the peak for H-Y should represent the size of the supercages (1.3 nm). The

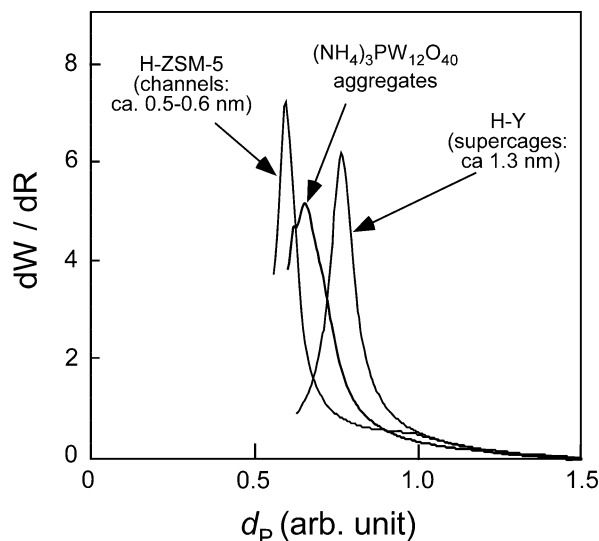


Figure 5. Horvath–Kawazoe pore size analysis based on Ar adsorption isotherms.

pore diameter of $(\text{NH}_4)_3\text{PW}_{12}\text{O}_{40}$ was considered to be ca. 1 nm (midway between 0.6 and 1.3 nm). This value is reasonably close to the size of the polyanion (1 nm), because the micropores or continuous voids in the single crystals should exist as neighboring vacancies of polyanions (and cations). The characteristic dodecahedral shape of the nanocrystallites is closely related to the crystal orientation of $(\text{NH}_4)_3\text{PW}_{12}\text{O}_{40}$ in a dodecahedron, where all the rhombic faces are parallel to the equivalent crystal planes, such as (110), (101), and so on, as illustrated in figure 6. The factors governing the outer shape of the $(\text{NH}_4)_3\text{PW}_{12}\text{O}_{40}$ (dodecahedra) may be the difference in surface energy and/or growth rates between the crystal planes, and may be similar to those for single crystals.

Okuhara *et al.* reported careful investigations on the microporosity of $\text{Cs}_{3-x}\text{H}_x\text{PW}_{12}\text{O}_{40}$, and proposed that the micropores in $\text{Cs}_{3-x}\text{H}_x\text{PW}_{12}\text{O}_{40}$ are formed with a crystallographic misfit and exist at the boundaries of closely attached nanocrystallites. The Okuhara model explains well the carefully determined micropore diameter and volumes, and is consistent with the small L_{XRD} values obtained for the corresponding Cs acidic salts [36,37]. This demonstrates that the boundaries between the nanocrystallites are not epitaxially connected, and that the nanocrystallites are incoherent in terms of X-ray diffraction. We also observed that when $\text{Cs}_3\text{PW}_{12}\text{O}_{40}$ was prepared at elevated temperature (368 K), spherical aggregates formed and the mesoporosity disappeared. The L_{XRD} for $\text{Cs}_3\text{PW}_{12}\text{O}_{40}$, on the other hand, was very much shorter (24 nm) than that for the $(\text{NH}_4)_3\text{PW}_{12}\text{O}_{40}$ (150 nm) prepared under the same conditions [23]. These results indicated that the “epitaxial connections” at the $\text{Cs}_3\text{PW}_{12}\text{O}_{40}$ crystallite boundaries were poorly developed even for the samples

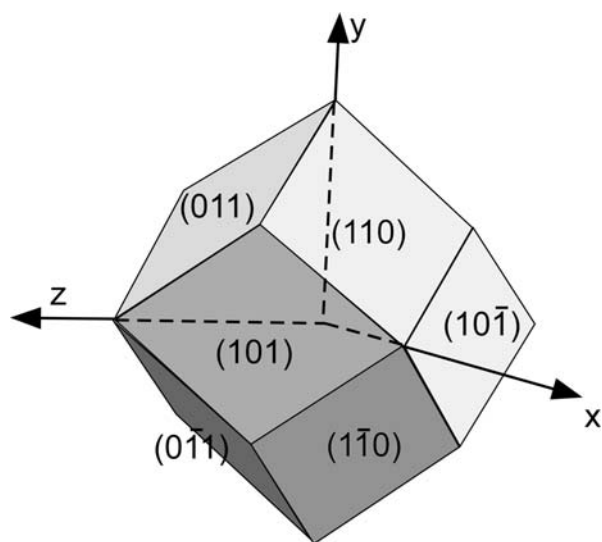


Figure 6. Relationship between the dodecahedral shape and crystal planes of $(\text{NH}_4)_3\text{PW}_{12}\text{O}_{40}$.

prepared at 368 K, which is probably due to the lower solubility of $\text{Cs}_3\text{PW}_{12}\text{O}_{40}$ compared to $(\text{NH}_4)_3\text{PW}_{12}\text{O}_{40}$.

5. Process of epitaxial self-assembly in the homogeneous precipitation method [21,22]

In order to elucidate the process of epitaxial self-assembly in more detail, we adopted the homogeneous precipitation method (HP method), which is based on the hydrolysis of urea as described below. Aqueous solutions of $\text{H}_3\text{PW}_{12}\text{O}_{40}$ and urea were heated at 373 K for various aging times. Here, the urea was hydrolyzed to form NH_4^+ cations in the $\text{H}_3\text{PW}_{12}\text{O}_{40}$ acidic solution, in accordance with the equation:



This method produced NH_4^+ ions, accompanied by CO_2 evolution throughout the solution, subsequently followed by complete decomposition such that nothing but NH_4^+ remained. This method was adopted because it becomes much simpler than the titration method discussed in the previous section. The structures of the products obtained for various aging times were monitored by SEM, nitrogen adsorption, X-ray powder diffraction, and solid state NMR.

The HP method produced dodecahedral aggregates similar to those prepared by the titration method. Using SEM, it was possible to monitor the changes to the outer shape of these aggregates during aging (images not shown). As schematically illustrated in figure 7, it was observed that spherical aggregates formed first, which were then transformed to dodecahedral shapes during aging. The following are the SEM observation results. For an aging (or heating) time of 3 h, aggregates of 1.5 μm in diameter were formed, where the outer shape was observed to be spherical rather than dodecahedral (figure 7c). At higher magnification, the as-formed nanocrystallites (5–10 nm in diameter) appeared loosely aggregated, with spaces between the crystallites that could be considered as mesopores. For the 12 h-aged sample, the aggregates had transformed into a dodecahedral shape with dulled edges, which became noticeably sharper after a further 12 h aging (midway of figure 7c and d). The 24 h-aged sample had a dodecahedral shape with sharp edges (figure 7d).

Table 2 shows the properties of the samples prepared using the HP method. The SEM results corresponded well to the pore properties determined by nitrogen adsorption, electron diffraction, and X-ray diffraction line width analysis (L_{XRD}): (i) SEM showed that the 3 h-aged sample consist of loosely assembled nanocrystallites, and accordingly nitrogen adsorption isotherms (not shown) indicated that the 3-h aged sample consisted of both mesopores and micropores, where the mesopores were considered as spaces between the loosely assembled nanocrystallites (figure 7c). Electron diffrac-

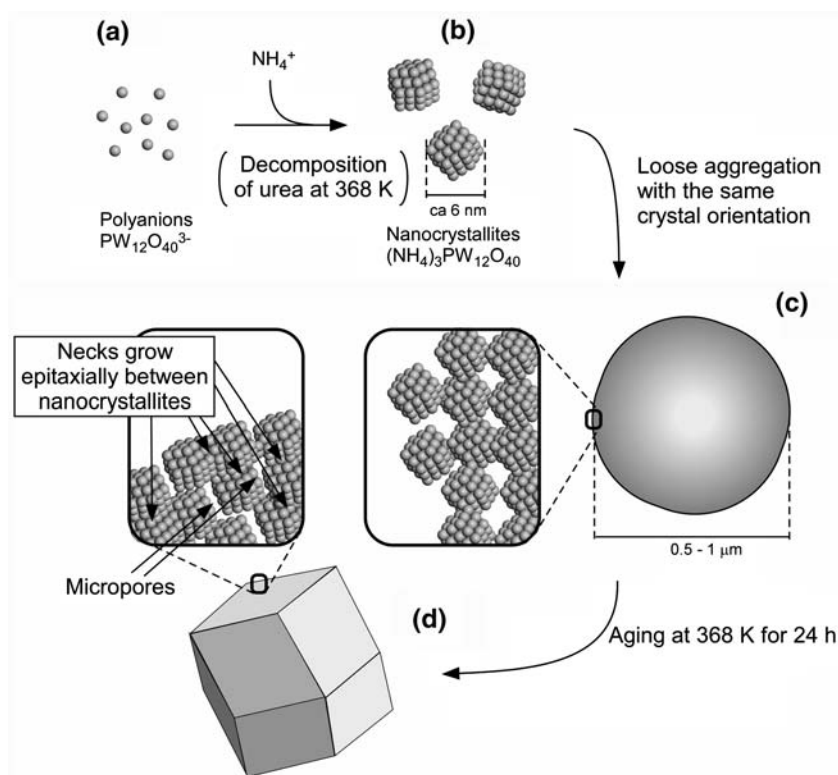


Figure 7. Schematic illustration of the formation process (via the HP method) of $(\text{NH}_4)_3\text{PW}_{12}\text{O}_{40}$ aggregates as “sponge crystals.”

tion patterns for a 3 h-aged spherical aggregate revealed that the nanocrystallite orientation was well ordered at an early stage in the formation process. Here, the L_{XRD} value was determined as 58 nm, indicating that epitaxial connections were formed to some extent between the nanocrystallites (table 2 and figure 7c). (ii) SEM showed that 24-h aged sample had dodecahedral shape with sharp edges, and accordingly the sample gave L_{XRD} as large as 260 nm and spotted ED patterns like a single crystal. The sample consisted of only micropores (figure 7d).

According to SEM, ED, X-ray diffraction, and N_2 adsorption, the formation process is envisaged as follows: at the initial nucleation stage, spherical aggregates with meso- and micro-pores and low crystallinity, are formed together with very fine particles. During the growth (aggregation) stage and as the precipitation reaction progresses, these spheres in which the nanocrystallites loosely self-assemble, grow gradually into

regular, microporous, highly crystalline, and rigid dodecahedra.

6. “Mesocrystals,” a category of self-assembled crystallites proposed by Cölfen and Antonietti

Cölfen and Antonietti described “mesocrystals” as oriented superstructures of nanocrystals with common outer faces, formed from nonspherical, crystalline building units [24]. According to the review, a schematic illustration is drawn in figure 8. Many compounds and materials form mesocrystals, depending on the preparation conditions. Mesocrystals often show characteristic outer shapes reflecting the ordered crystal orientation of the constituent nanocrystallites. Cölfen and Antonietti categorized these mesocrystals into specific groups, depending on whether they were prepared in the absence or presence of additives used to temporarily stabilize the nanocrystallites. Surface-active agents such as double hydrophilic block copolymers, are typical additives used to control the growth and aggregation of nanocrystallites. By using these additives, it is possible to temporarily halt the self-organization process midway, resulting in the formation of an intermediate species or “mesocrystal,” in which the primary unit can still be identified. Cölfen and Antonietti highlighted several examples of mesocrystals, including those of CeO_2 , CuO , CaCO_3 , $\alpha\text{-Fe}_2\text{O}_3$, $\text{CoC}_2\text{O}_4 \cdot 2\text{H}_2\text{O}$ and other organic and inorganic compounds.

Table 2
Properties of $(\text{NH}_4)_3\text{PW}_{12}\text{O}_{40}$ prepared by the HP method (Ref. 21)

Aging time (h)	BET surface area ($\text{m}^2 \text{g}^{-1}$)	d_{BET} (nm)	Pore volume ($10^{-2} \text{cm}^3 \text{g}^{-1}$)	L_{XRD} (nm)	$L_{\text{XRD}}/d_{\text{BET}}$
3	81	12	5.1	58	4.8
6	74	13	5.5	270	21
12	64	15	3.5	260	17
24	49	20	2.5	260	13

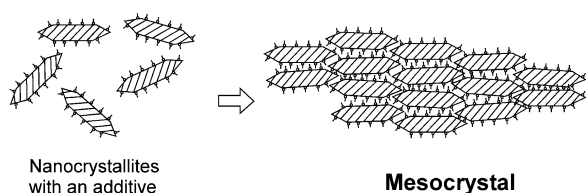


Figure 8. Schematic illustration representing the typical formation of a mesocrystal discussed by Cölfen and Antonietti in ref. 24. Non-spherical nanocrystallites self-assemble with ordered orientation to form large aggregates, either with or without the presence of certain additives.

Cölfen and Antonietti described in the review that mesocrystals are also “examples of non-classical crystallization, a mechanism which proceeds not via ion-by-ion attachment, but by a modular nanobuilding-block route” [24]. In terms of the formation process, Cölfen and Antonietti categorized the $(\text{NH}_4)_3\text{PW}_{12}\text{O}_{40}$ dodecahedra as an example of “mesocrystals.”

7. Definition of a new category of porous crystals: “sponge crystals”

The category “mesocrystals” is a concept focusing on the formation process that includes nanocrystallites aggregation. A new concept is needed to describe the final structure of $(\text{NH}_4)_3\text{PW}_{12}\text{O}_{40}$ as a characteristic porous single crystal. Here, we propose a new category of porous single crystals referred to as “Sponge crystals.” “Sponge crystals” are defined as single crystals having continuous voids within them, and unlike zeolites, no intrinsic structural pores (figure 9). In order to comply with this definition for “sponge crystals,” the crystal structures of a compound should not have

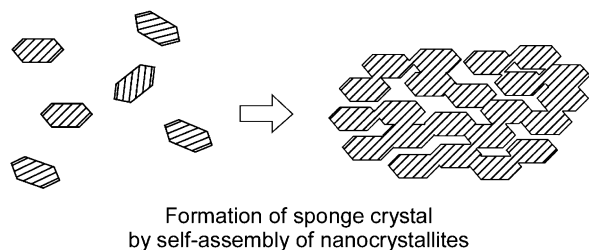
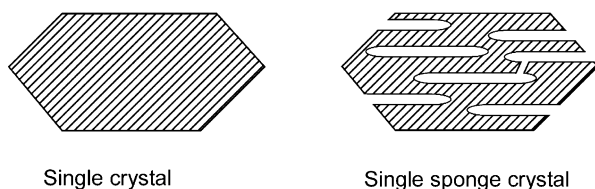


Figure 9. “Sponge crystal.” Schematic illustration of the definition and a likely formation mechanism by self-assembly of nanocrystallites.

intrinsic structural pores defined by the crystal structure itself, therefore ruling out zeolites as a class of “sponge crystal.” An ideal “sponge crystal” takes the form shown in the top part of figure 9. Continuous voids in a single crystal result in pores being formed in the crystal; leading to the term “sponge crystal.” It should be noted that “sponge crystals” are not always soft nor elastic, as the term “sponge” is commonly used for porous brittle substances like “zirconium metal sponge.”

This new category includes molecular single crystals having continuous voids originating from the neighboring vacancies (≥ 1 nm) of the constituent large molecules, affording nanospaces in the crystals. Here, the whole crystal maintains an ordered structure as a single crystal, while the vacancies define the microporosity. In the crystalline state, a sponge crystal is highly coherent in terms of diffraction, as confirmed by the powder X-ray diffraction technique.

A likely mechanism for the formation of sponge crystals occurs through self-assembly of the nanocrystallites, to form strongly inter-connected nanocrystallites leaving residual voids or micropores between them (figure 9, bottom).

Figure 10 and table 3 represents the relationship among the concepts of sponge crystals, mesocrystals, and porous crystals. Porous crystals like zeolites and aluminophosphates, are essentially single crystals comprising pores within them. Since sponge crystals are also considered as porous single crystals (figure 9), we conclude that these two crystal types belong to the same category (Porous crystals). The difference between sponge crystals and zeolites are that the pores of the former are not intrinsic structural pores (“built-in” pores; compare figures 9 and 11). In this context, the usual porous crystals such as zeolites may be called “intrinsic porous crystals” (table 3). On the other hand, in terms of the formation mechanism, some sponge crystals are formed by self-assembly of the nanocrystallites, and accordingly they are categorized as mesocrystals. Some sponge crystals on the other hand, are not thought to be formed by nanocrystallite aggregation, and are therefore not regarded as mesocrystals (e.g. $\text{Cs}_4\text{PMO}_{11}\text{VO}_{40}$).

8. $(\text{NH}_4)_3\text{PW}_{12}\text{O}_{40}$ as a member of the “mesocrystal” family

In terms of the formation process, porous $(\text{NH}_4)_3\text{PW}_{12}\text{O}_{40}$ is considered to be a member of the mesocrystal family. In their preparation, the nanocrystallites form and then self-assemble into aggregates having ordered structure. As a result, the aggregates have a symmetrical dodecahedral shape, which is closely related to the crystal orientation of the constituent nanocrystallites. These features represent well the characteristics of the mesocrystals highlighted by Cölfen and

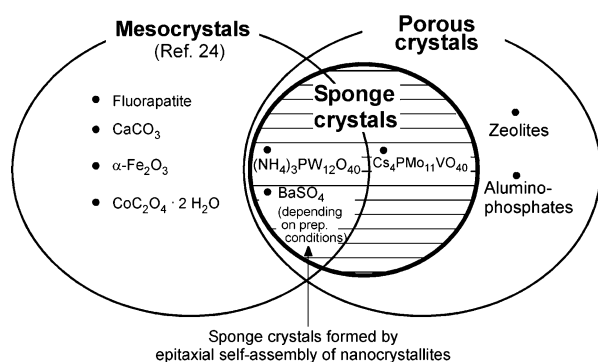


Figure 10. Relationship among the concepts of sponge crystals, mesocrystals and porous crystals. Porous crystals are classified into two category: Usual porous crystals like zeolites have intrinsic structural pores (“built-in” pores). The pores in “sponge crystals” are not intrinsic structural pores. Some “sponge crystals” such as $(\text{NH}_4)_3\text{PW}_{12}\text{O}_{40}$ are formed by aggregation of nanocrystallites, and are accordingly classified as “mesocrystals.”

Antonietti. In terms of the final structure however, the product has a structure very different from that of other “mesocrystals.” Most of the mesocrystals described by Cölfen and Antonietti have an ordered crystal orientation of the constituent nanocrystallites. However, from a crystallographic viewpoint, these mesocrystals are still aggregates of discrete nanocrystallites. On the other hand, each porous dodecahedral aggregate of $(\text{NH}_4)_3\text{PW}_{12}\text{O}_{40}$ have an ordered structure as a single crystal. In this context, $(\text{NH}_4)_3\text{PW}_{12}\text{O}_{40}$ may be considered a special example of a “mesocrystal.”

9. $(\text{NH}_4)_3\text{PW}_{12}\text{O}_{40}$ as a member of the novel class of porous single crystals: “Sponge crystals”

As shown in figures 9 and 11, from the viewpoint of porous crystal structures, $(\text{NH}_4)_3\text{PW}_{12}\text{O}_{40}$ is very different from the well-known microporous crystals such as zeolites and aluminophosphates. The well-known microporous crystals have an intrinsic structural micropore network defined by their crystal structure (“built-in” pores), while $(\text{NH}_4)_3\text{PW}_{12}\text{O}_{40}$ has none. The micropores in $(\text{NH}_4)_3\text{PW}_{12}\text{O}_{40}$ are very probably continuous vacancies of the molecules (polyanions and

cations). The continuous vacancies originate from residual spaces between the constituent nanocrystallites.

Unlike zeolites, which comprise pores defined by their crystal structure, the shape of the $(\text{NH}_4)_3\text{PW}_{12}\text{O}_{40}$ pores in principle, adopts various connectivities or networks in the $(\text{NH}_4)_3\text{PW}_{12}\text{O}_{40}$ crystal. In this context, a new concept “sponge crystals” is needed to discriminate the features of the porous $(\text{NH}_4)_3\text{PW}_{12}\text{O}_{40}$ “single crystals,” from those of typical microporous crystals (figures 9 and 11). This characteristic feature evokes the structure of sponges, which have pore networks with apparently random shape. Here, we conclude that $(\text{NH}_4)_3\text{PW}_{12}\text{O}_{40}$ is a “sponge crystal.”

The characteristics of “sponge crystals” provide a future possibility that allow us to design various connectivity of the micropore network in single crystals of $(\text{NH}_4)_3\text{PW}_{12}\text{O}_{40}$, which may open a new chemistry of designing pore structures in solids as materials for adsorbents and catalysts.

10. Other examples of “sponge crystals” reported in the literature

Another example of “sponge crystals” is porous $\text{Cs}_4\text{PMo}_{11}\text{VO}_{40}$ reported by Schlögl *et al.* Here, Schlögl *et al.* supposed the micropores to be vacancies of only polyanions [41]. The polyanions are tetravalent and the cation:anion ratio is 4:1. However, this compound took the same cubic crystal structure as that of $(\text{NH}_4)_3\text{PW}_{12}\text{O}_{40}$, which has a cation:anion site ratio of 3:1. They concluded that the vacancies generated in one-fourth of the anion sites, like $\text{Cs}_3[\text{PMo}_{11}\text{VO}_{40}]_{(3/4)}$, are generated in order to maintain the chemical composition and charge neutrality. In addition to epitaxial self-assembly, the method outlined above is tentatively considered another mechanism for the formation of “sponge crystals” (figure 10).

Judat and Kind reported that BaSO_4 , which is considered a typical compound formed by the ion-by-ion mechanism, also grows like $(\text{NH}_4)_3\text{PW}_{12}\text{O}_{40}$ under certain conditions [42], representing another example of the epitaxial self-assembly mechanism. Using TEM, they confirmed that BaSO_4 has several pores within its crystal, and as such, it can also be considered to meet the

Table 3
Concepts of “sponge crystals,” usual microporous crystals and “mesocrystals”

Category	Pores	Ordered structure as a single crystal	Formation process	Examples
Sponge crystal	Continuous voids. Not intrinsic structural pores	Required	Any	$(\text{NH}_4)_3\text{PW}_{12}\text{O}_{40}$, $\text{Cs}_4\text{PMo}_{11}\text{VO}_{40}$, BaSO_4 (Ref. 42)
Usual (intrinsic) porous crystal	Intrinsic structural pores. (“Bult-in” pores.)	Required	Any	Zeolites
Mesocrystal (Ref. 24)	Not required	Not required	Nanocrystallites aggregation in a regular manner	CaCO_3 , $(\text{NH}_4)_3\text{PW}_{12}\text{O}_{40}$, BaSO_4 (Ref. 42)

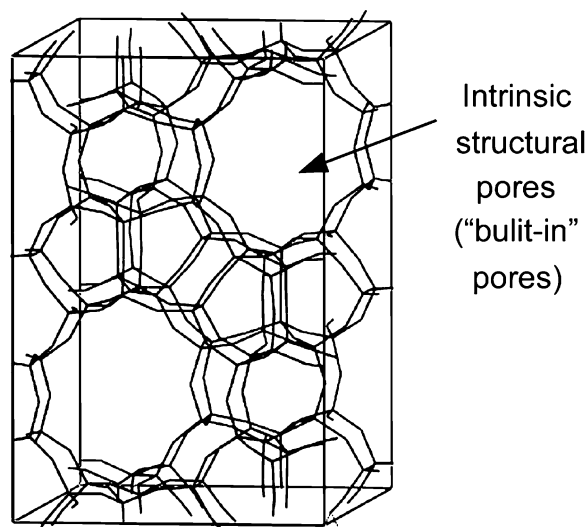


Figure 11. Illustration of the intrinsic pores (“built-in pores”) of zeolites.

same definition of “sponge crystal.” However, the observed pores in BaSO_4 were in fact closed, and the actual porosity and surface area of the BaSO_4 are low. On the other hand, the $(\text{NH}_4)_3\text{PW}_{12}\text{O}_{40}$ described here show high surface area and porosity, as shown in tables 1 and 2. These results demonstrate that $(\text{NH}_4)_3\text{PW}_{12}\text{O}_{40}$ have a microporous and continuous surface that is accessible to gas molecules from outside of the crystal.

11. Conclusions

Here we propose a novel class of porous single crystals: “Sponge crystals” are defined as single crystals having continuous voids within them, but unlike zeolites, no intrinsic structural pores. It should be noted that “sponge crystals” are not always soft nor elastic, as the term “sponge” is commonly used for porous brittle substances like “zirconium metal sponge.” To be considered a “sponge crystal,” it is essential that their crystal structure should not have intrinsic structural pores built into it. “Epitaxial self-assembly” (Ito, Inumaru, and Misono, *J. Phys. Chem. B* 101 (1997) 9958) is a mechanism which forms sponge crystals, as previously reported for porous $(\text{NH}_4)_3\text{PW}_{12}\text{O}_{40}$. In this case, we demonstrated that $(\text{NH}_4)_3\text{PW}_{12}\text{O}_{40}$ microporous dodecahedra are formed by nanocrystallites, all self-assembling with the same crystal orientation, and interconnected by necks epitaxially grown between the nanocrystallites. The formation process may be included in the recently proposed comprehensive concept of “mesocrystals,” which describes the formation of large aggregates by the ordered assembly of inorganic nanocrystallites. In terms of the final structure however, $(\text{NH}_4)_3\text{PW}_{12}\text{O}_{40}$ has a structure very different from those of other “mesocrystals.” Indeed, most of the

mesocrystals described by Cölfen and Antonietti have the same ordered crystal orientation as the constituent nanocrystallites, which from a crystallographic viewpoint, are still aggregates of discrete nanocrystallites. Furthermore, mesocrystals are not necessarily porous. Although $(\text{NH}_4)_3\text{PW}_{12}\text{O}_{40}$ has no “built in” pores in the crystal structure, the aggregates are microporous and have an ordered structure as single crystals. The final structure should consequently be classified as a novel type of porous single crystal category, totally different from the typical porous crystals such as zeolites and aluminophosphates. The $(\text{NH}_4)_3\text{PW}_{12}\text{O}_{40}$ micropores can be regarded as continuous vacancies of the molecules (anions and cations) in the dodecahedra, having ordered structure as single crystals. In summary, we conclude that $(\text{NH}_4)_3\text{PW}_{12}\text{O}_{40}$ represents an example of “sponge crystals.”

Acknowledgment

This account is based on the previous study, which was done at the University of Tokyo under the supervision of Prof. Makoto Misono and cooperation of Dr. Takeru Ito. This work was partially supported by a Grant-in-Aid from the Japan Ministry of Education for Science, Culture, Sports and Technology (MEXT), and a CREST project from the Japan Science and Technology Corporation (JST). The author thanks Dr. A. Toriki (Sumitomo 3M) for useful discussion.

References

- [1] C.B. Murray, C.R. Kagan and M.G. Bawendi, *Ann. Rev. Mater. Sci.* 30 (2000) 545.
- [2] H. Cölfen and S. Mann, *Angew. Chem. Int. Ed.* 42 (2003) 2350.
- [3] A. Stein and R.C. Schroden, *Curr. Opin. Solid State Mater. Sci.* 5 (2001) 553.
- [4] O.D. Velev, T.A. Jade, R.F. Lobo and A. M. Lenhoff, *Nature* 389 (1997) 447.
- [5] W. Luck, M. Klier and H. Wesslau, *Ber. Bunsen-Ges. Phys. Chem.* 67 (1963) 75.
- [6] N.V. Dzionkina and G.J. Vancso, *Soft Matter* 1 (2005) 265.
- [7] R. Schlögl and S.B. Abd Hamid, *Angew. Chemie Int. Ed.* 43 (2004) 1628.
- [8] T.J. Barton, L.M. Bull, W.G. Klemperer, D.A. Loy, B. McEnaney, M. Misono, P.A. Monson, G. Pez, G.W. Scherer, J.C. Vartuli and O.M.K. Yaghi, *Chem. Mater.* 11 (1999) 2633.
- [9] M. Misono, *Catal. Rev.-Sci. Eng.* 29 (1987) 269; 30 (1988) 339.
- [10] T. Okuhara, M. Mizuno and M. Misono, *Adv. Catal.* 41 (1996) 113.
- [11] N. Mizuno and M. Misono, *Chem. Rev.* 98 (1998) 199.
- [12] M. Misono, *Chem. Commun.* (2001) 1141.
- [13] S. Tatematsu, H. Hibi, T. Okuhara, and M. Misono, *Chem. Lett.* (1984) 865.
- [14] T. Okuhara, A. Kasai, N. Hayakawa, Y. Yoneda and M. Misono, *J. Catal.* 83 (1983) 121.
- [15] T. Okuhara, H. Watanabe, T. Nishimura, K. Inumaru and M. Misono, *Chem. Mater.* 12 (2000) 2230.
- [16] T. Okuhara, T. Nishimura, and M. Misono, *Chem. Lett.* (1995) 155.

- [17] T. Ito, K. Inumaru and M. Misono, *J. Phys. Chem. B.* 101 (1997) 9958.
- [18] K. Inumaru, H. Nakajima, T. Ito, M. Misono, *Chem. Lett.* (1996) 559.
- [19] M. Misono and K. Inumaru, JP1997-124311.
- [20] T. Ito, I.-K. Song, K. Inumaru, and M. Misono, *Chem. Lett.* (1997) 727.
- [21] T. Ito, K. Inumaru and M. Misono, *Chem. Mater.* 13 (2001) 824.
- [22] T. Ito, K. Inumaru and M. Misono, *Chem. Lett.* (2000) 830.
- [23] K. Inumaru, T. Ito and M. Misono, *Micropor. Mesopor. Mater.* 21 (1998) 629.
- [24] H. Cölfen and M. Antonietti, *Angew. Chem. Int. Ed.* 44 (2005) 5576.
- [25] T. Okuhara, *Chem. Rev.* 102 (2002) 3641.
- [26] Y. Yoshinaga, K. Seki, T. Nakato and T. Okuhara, *Angew. Chem. Int. Ed. Engl.* 36 (1997) 2833.
- [27] Y. Yoshinaga and T. Okuhara, *J. Chem. Soc., Faraday Trans.* 94 (1998) 2235.
- [28] T. Okuhara, T. Yamada, K. Seki, K. Johkan and T. Nakato, *Micropor. Mesopor. Mater.* 21 (1998) 637.
- [29] T. Yamada, Y. Yoshinaga and T. Okuhara, *Bull. Chem. Soc. Jpn.* 71 (1998) 2727.
- [30] Y. Yoshinaga, K. Seki, T. Nakato and T. Okuhara, *Angew. Chem. Int. Ed. Engl.* 36 (1997) 2833.
- [31] T. Okuhara, T. Yamada, K. Seki, K. Johkan and T. Nakato, *Micropor. Mesopor. Mater.* 21 (1998) 637.
- [32] T. Okuhara and T. Nakato, *Catal. Surv. Jpn.* 2 (1999) 31.
- [33] T. Yamada, K. Johkan and T. Okuhara, *Micropor. Mesopor. Mater.* 26 (1998) 109.
- [34] M. Yosihmune, Y. Yoshinaga, T. Okuhara, *Chem. Lett.* (2002) 330.
- [35] T. Yamada, Y. Yoshinaga and T. Okuhara, *Bull. Chem. Soc. Jpn.* 71 (1998) 2727.
- [36] Y. Yoshinaga, T. Suzuki, M. Yoshimune and T. Okuhara, *Top. Catal.* 19 (2002) 179.
- [37] T. Okuhara, *Appl. Catal. A: Gen.* 256 (2003) 213.
- [38] S.T. Gregg and M.M. Tayyab, *J. Chem. Soc., Faraday Trans., I* 74 (1978) 348.
- [39] J. B. McMonagle and J.B. Moffat, *J. Colloid Interface Sci.* 101 (1984) 479.
- [40] D. Lapham and J.B. Moffat, *Langmuir* 7 (1991) 2273.
- [41] S. Berndt, D. Herein, F. Zemlin, E. Beckmann, G. Weinberg, J. Schütze, G. Mestl and R. Schlögl, *Ber. Bunsen-Ges. Phys. Chem.* 102 (1998) 763.
- [42] B. Judat and M. Kind, *J. Colloid Interface Sci.* 269 (2004) 341.